



# Identification of two novel heterodimeric ABC transporters in melanoma: ABCB5 $\beta$ /B6 and ABCB5 $\beta$ /B9

Received for publication, April 28, 2023, and in revised form, November 18, 2023 Published, Papers in Press, December 23, 2023,  
<https://doi.org/10.1016/j.jbc.2023.105594>

Louise Gerard<sup>1</sup>, Laurent Duvivier<sup>1</sup>, Marie Fourrez<sup>1</sup>, Paula Salazar<sup>2</sup> , Lindsay Sprimont<sup>1</sup>, Di Xia<sup>2</sup>,  
Suresh V. Ambudkar<sup>2</sup>, Michael M. Gottesman<sup>2</sup>, and Jean-Pierre Gillet<sup>1,\*</sup> 

From the <sup>1</sup>Laboratory of Molecular Cancer Biology, URPhyM, NARILIS, University of Namur, Namur, Belgium; <sup>2</sup>Laboratory of Cell Biology, Center for Cancer Research, National Cancer Institute, National Institutes of Health, Bethesda, Maryland, USA

Reviewed by members of the JBC Editorial Board. Edited by Kirill Martemyanov

ABCB5 is a member of the ABC transporter superfamily composed of 48 transporters, which have been extensively studied for their role in cancer multidrug resistance and, more recently, in tumorigenesis. ABCB5 has been identified as a marker of skin progenitor cells, melanoma, and limbal stem cells. It has also been associated with multidrug resistance in several cancers. The unique feature of ABCB5 is that it exists as both a full transporter (ABCB5FL) and a half transporter (ABCB5 $\beta$ ). Several studies have shown that the ABCB5 $\beta$  homodimer does not confer multidrug resistance, in contrast to ABCB5FL. In this study, using three complementary techniques, (1) nanoluciferase-based bioluminescence resonance energy transfer, (2) coimmunoprecipitation, and (3) proximity ligation assay, we identified two novel heterodimers in melanoma: ABCB5 $\beta$ /B6 and ABCB5 $\beta$ /B9. Both heterodimers could be expressed in High-Five insect cells and ATPase assays revealed that both functional nucleotide-binding domains of homodimers and heterodimers are required for their basal ATPase activity. These results are an important step toward elucidating the functional role of ABCB5 $\beta$  in melanocytes and melanoma.

ABCB5 is an ABC transporter that is a member of one of the largest, most ancient superfamilies of proteins found in all living organisms. Mammalian ABC proteins are classified into seven families from A to G based on sequence homology (1). In humans, ABC transporters are mostly exporters, with the exception of ABCA4 (2) and ABCD4 (3), which are importers. They exist either as full transporters with two transmembrane domains (TMDs) and two nucleotide-binding domains (NBDs) or as half transporters with one TMD and one NBD, which must either homodimerize or heterodimerize to become functional. However, not all are transporters. ABCE and ABCF members exist as twin NBDs without TMDs and are involved in mRNA translation control (4). The ABCC family includes ABCC7, an ATP-gated chloride channel that is also known as the cystic fibrosis transmembrane conductance regulator (5), while ABCC8 and ABCC9 serve as regulatory subunits of the ATP-sensitive potassium channel (Kir6.x) (6).

ABCB5 has been highlighted as a marker of skin progenitor cells (7), melanoma stem cells (8), and, more recently, limbal stem cells (9). It has also been reported to be a mediator of multidrug resistance in melanoma (10), breast cancer (11), colorectal cancer (12, 13), hepatocellular carcinoma (14), and several hematological malignancies (15, 16). Despite these reports, characterization of ABCB5 remains minimal. Several transcripts of human *ABCB5* have been identified and transcribed from at least two different promoters, as reported in the Zenbu genome browser. According to the AceView program, which provides a strictly complementary deoxyribonucleic acid (cDNA)-supported view of the human transcriptome and genes, *ABCB5* gene transcription gives rise to at least 11 different transcript variants (17). Among these, three variants have been documented: ABCB5.b (7) (812 aa, also referred to as ABCB5 $\beta$ ), ABCB5.h (18) (131 aa, also referred to as ABCB5 $\alpha$ ), and ABCB5.a (19) (1257 aa, also referred to as ABCB5FL full-length).

ABCB5 $\beta$  was predicted to have a TMD composed of six  $\alpha$ -helices flanked by two intracellular NBDs (20). Conventional half transporters possess only one NBD, either at the N- or the C-terminal region (21). The ABCB5 $\beta$  N-terminal NBD lacks the Walker A motif, which precludes the binding of ATP. However, ABCB5 $\beta$  could dimerize to form a functional transporter. Potential dimerization motifs have been identified in its N-terminal region (20). Nevertheless, it has been shown that an ABCB5 $\beta$  homodimer cannot confer drug resistance in either the yeast model *Saccharomyces cerevisiae* or in mammalian cells (19, 22). Since these studies focused on a limited number of drugs, we cannot exclude the possibility that this homodimer might be involved in drug resistance or biological functions that have yet to be unraveled. Yet, it is also worth considering that ABCB5 $\beta$  could dimerize with other half transporters of the ABCB family to become functional.

Interestingly, ABCB5 $\beta$  belongs to a family that comprises both full and half transporters. These latter include ABCB2/TAP1, ABCB3/TAP2, ABCB6, ABCB7, ABCB8, ABCB9/TAPL, and ABCB10. The first two, ABCB2 and ABCB3, are known to dimerize in the membrane of the endoplasmic reticulum (ER) to transport peptides from the cytoplasm into the ER lumen, where they associate with major histocompatibility complex class I molecules and are presented to T-lymphocytes

\* For correspondence: Jean-Pierre Gillet, [jean-pierre.gillet@unamur.be](mailto:jean-pierre.gillet@unamur.be).

## ABCB5 $\beta$ heterodimerizes with ABCB6 and ABCB9 in melanoma

(23). Furthermore, ABCB7 and ABCB10 have been shown to form a complex with ferrochelatase in the mitochondria, where they are involved in heme biosynthesis (24).

The three remaining half transporters have been linked to multidrug resistance in several cancer types, including melanoma (25–27). Bergam and colleagues demonstrated that ABCB6 is involved in the early steps of melanogenesis (28). Furthermore, mutations in this gene are responsible for dyschromatosis universalis hereditaria, a rare pigmentary genodermatosis (29). ABCB5 and ABCB8 have been proposed to play a role in the transport of melanin metabolites (30). These transporters could mediate the sequestration of toxic melanin metabolites into lysosomes or melanosomes, thereby protecting melanocytes. In melanoma, they could sequester drugs in these organelles (31). To date, no strong experimental evidence supports these conjectures. Considering that several ABCB half transporters form functional heterodimers, we hypothesized that ABCB5 $\beta$  might heterodimerize with other related members of the ABCB family, possibly, ABCB6, ABCB8, or ABCB9.

In this study, we identified two novel heterodimeric ABC transporters in melanoma, ABCB5 $\beta$ /B6 and ABCB5 $\beta$ /B9, using three complementary techniques: nanoluciferase-based bioluminescence resonance energy transfer (NanoBRET), coimmunoprecipitation (Co-IP), and proximity ligation assay (PLA). When ABCB5 $\beta$ /B6 and ABCB5 $\beta$ /B9 heterodimers were fused with the P-glycoprotein (P-gp, also named ABCB1) flexible linker region and expressed in High-Five insect cells, they exhibited significant levels of basal ATPase activity. This discovery paves the way for a better understanding of the roles played by these heterodimeric transporters in melanoma.

### Results

#### *NanoBRET assay reveals ABCB6 and ABCB9 as interacting partners of ABCB5 $\beta$*

We hypothesized that ABCB5 $\beta$  might heterodimerize with a half transporter of the ABCB family. A review of the literature, which shows ABCB2-ABCB3 and ABCB7-ABCB10 interaction, led us to select three half transporters, namely ABCB6, ABCB8, and ABCB9, as possible partners for ABCB5 $\beta$ . To study the putative interactions between ABCB5 $\beta$  and these proteins, we conducted a NanoBRET assay as described in Fig. S1. Each of the four proteins was tagged with either a NanoLuc-donor or HaloTag-acceptor at either the amino (N) or carboxy (C) terminus of the protein, resulting in 16 constructs and eight potential donor/acceptor combinations for each protein pair (Fig. S1B). For each combination to be tested, two constructs (one with NanoLuc and one with HaloTag) were transfected in HEK-293T cells and either the fluorescent NanoBRET HaloTag 618 ligand or a dimethyl sulfoxide (DMSO) vehicle was added to the cells. The NanoBRET NanoLuc substrate was then added, and donor and acceptor signals were measured, which allowed us to calculate a NanoBRET ratio by dividing the acceptor emission value by the donor emission value for each sample in both conditions. To factor in the donor-contributed background, we subtracted

the no-ligand control NanoBRET ratio (*i.e.*, DMSO vehicle) from the ligand-containing sample NanoBRET ratio to obtain the corrected NanoBRET ratio (Fig. S1B).

As controls for the assay, we also tested the interaction between additional ABC proteins. To this end, we tested the fully characterized ABCB2/B3 heterodimer as a positive control (23). Furthermore, we tested the putative interactions between ABCB2-ABCD1 and ABCB3-ABCD1 proteins as negative controls, since the ABCB2/B3 heterodimer is expressed in the ER membrane while ABCD1 is a peroxisomal transporter. As an additional control, we also looked for a possible interaction between ABCB5 $\beta$  and ABCD1 proteins.

Each tested protein pair yielded a high NanoBRET ratio for one or more donor/acceptor combinations, suggesting heterodimerization (Fig. S1B). Variations in the transfection efficiency of the donor and acceptor constructs or the constitutive expression of the proteins led to an environment in which the concentrations of all partners were not regulated, rendering any quantitative assumption difficult. As a result, in this experiment, the NanoBRET ratio was used as qualitative information. Ratios similar to the no-ligand negative control were classified as noninteracting, while ratios above that suggested heterodimerization.

It should be noted that a major drawback of resonance energy transfer assays (*e.g.*, FRET, BRET, and NanoBRET) is that a signal can be detected when proteins are in close proximity but do not interact together (32). This is typically the case for transmembrane proteins, as under overexpression conditions, membrane crowding may lead to protein aggregates in which donors and acceptors can transfer energy to one another without the generation of heterodimers. To overcome this limitation, we decided to decrease the amount of donor and acceptor constructs linearly. Nonspecific interaction should result in decreased NanoBRET ratios, while these ratios should remain stable if the interaction is specific.

For this experiment, we chose the best donor/acceptor combination based on the highest NanoBRET ratio (Fig. S1B). The absence or low signal in alternative tag combinations for a tested pair indicates that the tags might be either too far from one another to transfer energy, not correctly oriented, or might be impairing protein folding, localization, or dimerization (33). Therefore, the pair with the largest NanoBRET ratio represents the combination for which both tags are in the best conformation to transfer energy to one another. The selected pairs are highlighted in Fig. S1B.

HEK-293T cells were transfected with decreasing amounts of NanoLuc (donor) and HaloTag (acceptor) constructs ranging from 1  $\mu$ g to 0.125  $\mu$ g for each construct (Fig. 1). The NanoBRET ratio decreased, along with the DNA amount, for the ABCB2-ABCD1, ABCB3-ABCD1, and ABCB5 $\beta$ -ABCD1 pairs tested as negative controls (Fig. 1A) and stayed constant regardless of the amount of DNA transfected for ABCB2-ABCB3, which served as a positive control (Fig. 1B). Interestingly, NanoBRET ratios remained similar in all conditions for ABCB5 $\beta$ /B6 and ABCB5 $\beta$ /B9, suggesting that these proteins might form true heterodimers. The NanoBRET ratio

## ABCB5 $\beta$ heterodimerizes with ABCB6 and ABCB9 in melanoma

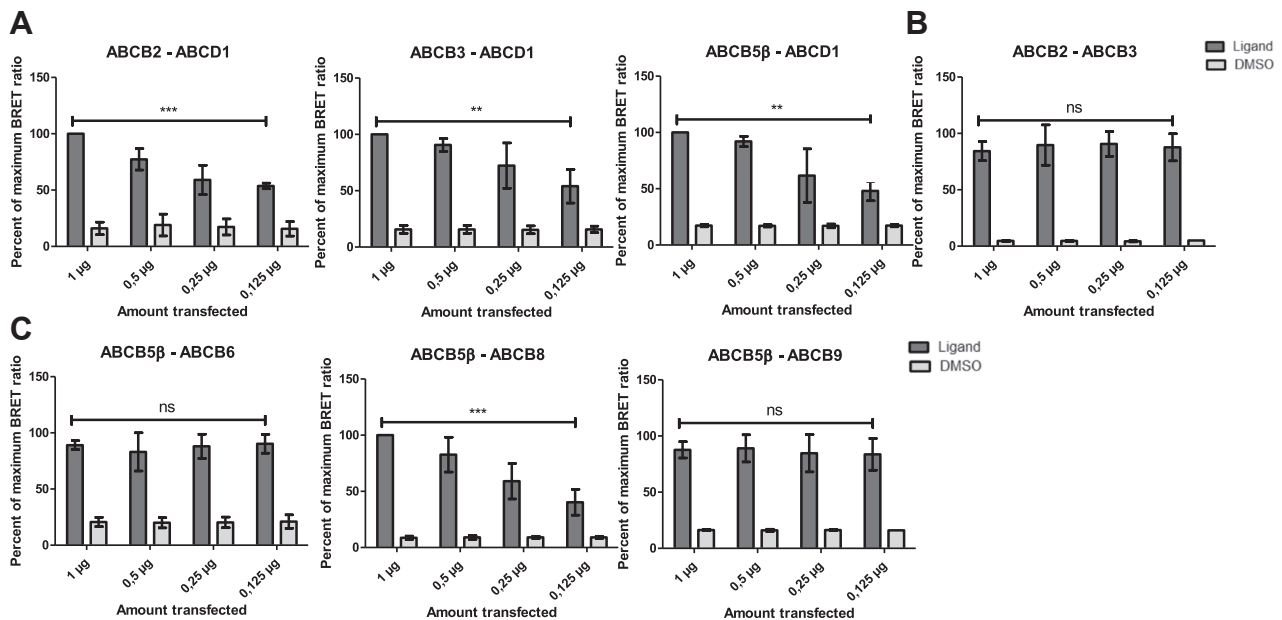


**Figure 1. NanoBRET dilution assay reveals two putative heterodimers, ABCB5 $\beta$ /B6, and ABCB5 $\beta$ /B9.** HEK-293T cells were transfected with decreasing amounts of NanoLuc and HaloTag constructs. Transfection started at 1  $\mu$ g and gradually decreased to 0.125  $\mu$ g per construct. DMSO refers to the technical negative control to which DMSO is added instead of ligand. Protein pairs serving as negative controls (ABCB2-ABCD1, ABCB3-ABCD1, ABCD1-ABCB5 $\beta$ ) (A) and a positive control pair (ABCB2-ABCB3) (B) were tested alongside ABCB5 $\beta$ -ABCB6, ABCB5 $\beta$ -ABCB8, and ABCB5 $\beta$ -ABCB9 (C). Data are presented as mean  $\pm$  SD. Simple linear regression was used to test whether the amount transfected significantly influenced the NanoBRET ratio ( $n = 3$ ).  $p$ -values are represented on graphs as \*\*\* $p < 0.001$ , \*\* $p < 0.01$ , and  $p > 0.05$ . For ABCB2-ABCD1 ( $R^2 = 0.8719$ ,  $F(1,10) = 68.07$ ), ABCB3-ABCD1 ( $R^2 = 0.6144$ ,  $F(1,10) = 15.94$ ), ABCB5 $\beta$ -ABCD1 ( $R^2 = 0.6661$ ,  $F(1,10) = 19.95$ ), and ABCB5 $\beta$ -ABCB8 ( $R^2 = 0.7526$ ,  $F(1,10) = 30.41$ ), the relation between both parameters was statistically significant. For ABCB2-ABCB3 ( $R^2 = 0.0269$ ,  $F(1,10) = 0.2767$ ), ABCB5 $\beta$ -ABCB6 ( $R^2 = 0.0011$ ,  $F(1,10) = 0.0113$ ), and ABCB5 $\beta$ -ABCB9 ( $R^2 = 0.0204$ ,  $F(1,10) = 0.2080$ ), changes in the amount of transfected DNA did not influence the NanoBRET ratio. DMSO, dimethyl sulfoxide; NanoBRET, nanoluciferase-based bioluminescence resonance energy transfer.

obtained for ABCB5 $\beta$ -ABCB8 decreased along with the amount of DNA transfected, similar to the data generated from protein pairs assessed as negative controls.

### Donor saturation assay confirms the specificity of the interaction between ABCB5 $\beta$ /B6 and ABCB5 $\beta$ /B9 protein pairs

To confirm the specific interaction of the ABCB5 $\beta$ -ABCB6 and ABCB5 $\beta$ -ABCB9 protein pairs and the false positive signals of the ABCB5 $\beta$ -ABCB8, ABCB2-ABCD1, ABCB3-ABCD1, and ABCB5 $\beta$ -ABCD1 protein pairs, a saturation assay was performed in HEK-293T cells (Fig. 2). In this experiment, the amount of donor construct was held constant, while the amount of acceptor construct was gradually increased. For this assay, the smallest concentrations of donor and acceptor showing heterodimerization were used. If the interaction between both proteins is specific, the NanoBRET signal will increase in a hyperbolic manner, reaching a plateau when all the donors are saturated with the acceptors and luminescence can no longer increase. On the other hand, for a nonspecific interaction, the signal will increase linearly with an increasing acceptor concentration (Fig. 2A). At these concentrations, the signal from a nonspecific interaction will not reach a plateau due to the lack of affinity between proteins.

We carried out this donor saturation assay on the ABCB2-ABCB3 protein pair used as a positive control and compared the data to that from the three protein pairs chosen as negative controls. As shown in Figure 2B, the NanoBRET signal was saturable for the ABCB2-ABCB3 protein pair, while a linear

increase was observed for the ABCB2-ABCD1, ABCB3-ABCD1, and ABCB5 $\beta$ -ABCD1 pairs. This supports the specificity of the interaction for the ABCB2-ABCB3 protein pair. The specificity of the interaction was then assessed for the three protein pairs of interest. The analysis of the data revealed a hyperbolic increase in the NanoBRET signal that eventually reached a plateau phase for both the ABCB5 $\beta$ -ABCB6 and ABCB5 $\beta$ -ABCB9 protein pairs, similar to what was observed for the positive control. On the contrary, the donor saturation assay further supported a nonspecific interaction between the ABCB5 $\beta$  and ABCB8 proteins (Fig. 2C).

### Co-IP and PLA confirm interactions in cells between the ABCB5 $\beta$ -ABCB6 and ABCB5 $\beta$ -ABCB9 heterodimers

Co-IP is considered one of the standard methods for identifying or confirming the occurrence of protein-protein interaction events. Because of this, as a first step, we used HEK-293T cells, which constitutively express ABCB6 and ABCB9. Since the expression of ABCB5 $\beta$  had not been demonstrated in this cell line, we transfected them with mCherry-tagged ABCB5 $\beta$  (Fig. S2). The proteins of interest were immunoprecipitated using either an anti-mCherry, ABCB5, ABCB6, or ABCB9 antibody, and the interacting partners were analyzed using Western blotting after SDS-PAGE using corresponding antibodies to show protein-protein interaction (Fig. S2). An isotype control was used to determine the specificity of the signal obtained in the Western blots.

## ABCB5 $\beta$ heterodimerizes with ABCB6 and ABCB9 in melanoma

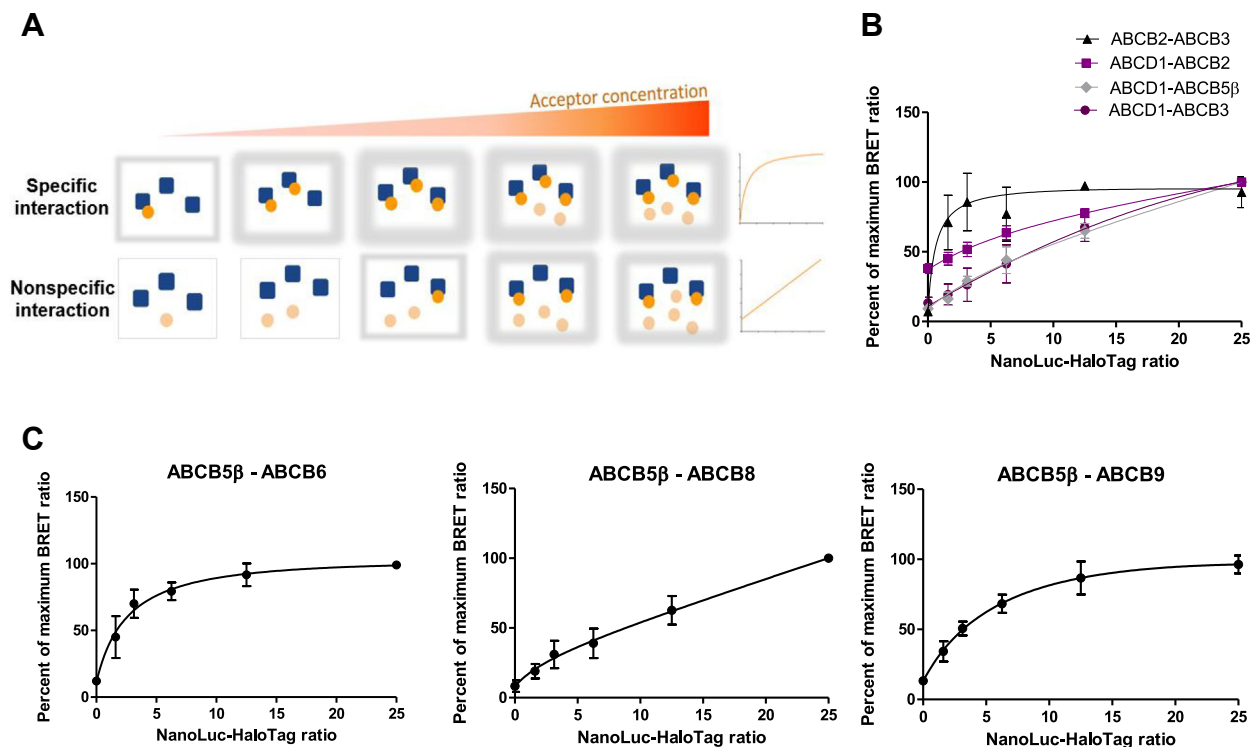


**Figure 2. Saturation assay confirms specific ABCB5 $\beta$ -ABCB6 and ABCB5 $\beta$ -ABCB9 interactions.** A, the concentration of the donor is held constant while the concentration of the acceptor is increased. If the interaction is specific, the signal will reach a plateau where all donors are saturated with acceptors, and luminescence will no longer increase. In the case of a nonspecific interaction, the signal will continue to increase linearly. For each square, the schematic *gray halo* represents the intensity of the NanoBRET signal observed from low to high. In graphs (B and C), the percent of the maximum NanoBRET ratio is plotted against the NanoLuc-HaloTag ratio. B, donor saturation assay for the positive control, ABCB2-ABCB3, and the negative controls, ABCB2-ABCD1, ABCB3-ABCD1, and ABCB5 $\beta$ -ABCD1. C, donor saturation assay for ABCB5 $\beta$ -ABCB6, ABCB5 $\beta$ -ABCB8, and ABCB5 $\beta$ -ABCB9. NanoBRET, nanoluciferase-based bioluminescence resonance energy transfer.

Membrane crowding, protein mislocalization, misfolding, and loss of function are some of the issues that might arise from membrane protein overexpression and the utilization of a tag. Therefore, we decided to work with Mel JuSo and UACC-257, two melanoma cell lines that constitutively express the target proteins (Fig. 3). Immunoprecipitation with either an anti-ABCB5, ABCB6, or ABCB9 antibody detects the

interacting partners, which were identified by Western blotting after an SDS-PAGE using the corresponding antibody. The data further supports the occurrence of interaction between the ABCB5 $\beta$ -ABCB6 and ABCB5 $\beta$ -ABCB9 protein pairs (Fig. 3).

*In situ* validation of the interactions for these two protein pairs was obtained using a PLA in both Mel JuSo and UACC-

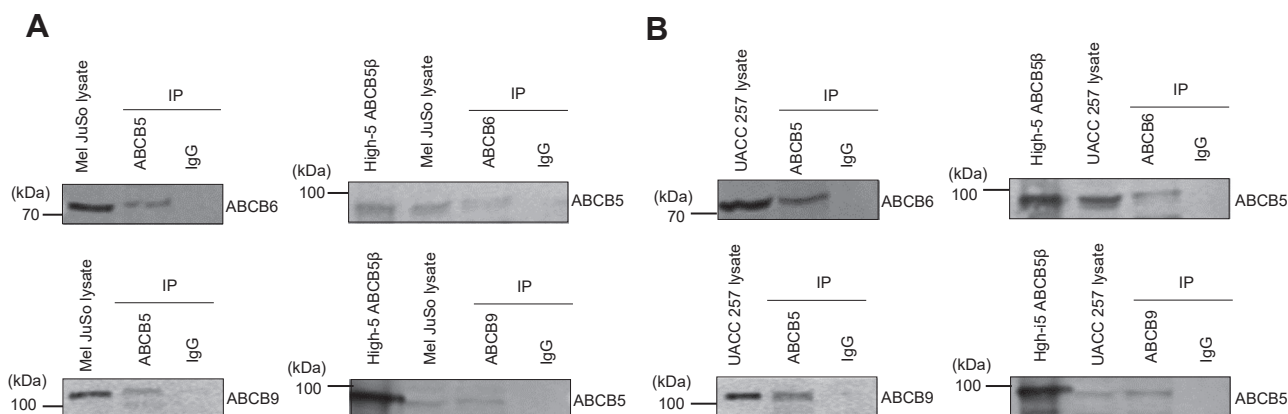


**Figure 3. Coimmunoprecipitation of ABCB5 $\beta$ -ABCB6 and ABCB5 $\beta$ -ABCB9 demonstrates the presence of these heterodimers in Mel JuSo and UACC-257 cells.** The Mel JuSo (A) or UACC-257 (B) proteins were immunoprecipitated (IP) with either an anti-ABCB5, anti-ABCB6, or anti-ABCB9 antibody. The precipitated proteins were revealed by Western blotting after SDS-PAGE using the corresponding antibody indicated on the *right side* of each blot. Fifteen micrograms of total proteins from the starting cell lysate were loaded in the first lane, while the total IP eluate was loaded on the gel. ABCB5 $\beta$  was expressed in High-Five insect cells, and total membrane proteins were prepared and loaded on the gel (High5 ABCB5 $\beta$ ) as a complementary molecular weight marker when using anti-ABCB5. An isotype control was performed to determine the specificity of the signal obtained in Western blot.

257 cells. A schematic image and explanation of the PLA process can be found in Fig. S3. Strong red PLA signals were detected for ABC5 $\beta$ -ABC6 and ABC5 $\beta$ -ABC9, indicating interactions between the studied protein pairs (Fig. 4A). To further assess the specificity of the PLA signal, multiple controls were performed. Biological controls were conducted in which Mel JuSo and UACC-257 cell lines were produced that stably expressed either a nontargeting shRNA or an ABC6-specific (or ABC9-specific) shRNA, resulting in the decrease of either ABC6 or ABC9 expression. Figure 4, B and C show the resulting decrease of expression at the mRNA and protein levels. In both cell lines, stable knockdown of either ABC6 or ABC9 resulted in a statistically significant decrease in PLA signal ( $p < 0.0001$ ) as compared to the nontargeting shRNA samples (Fig. 4D). Technical controls were also conducted in which just one of the two antibodies directed against the proteins of interest was added or neither was added (Fig. 4D).

**ABC5 $\beta$ /B6 and ABC5 $\beta$ /B9 linked with the P-gp linker exhibit basal ATPase activity**

Next, we wanted to determine whether ABC5 $\beta$ -ABC6 and ABC5 $\beta$ -ABC9 could hydrolyze ATP, which is required for the transport of substrates across membranes. Genetic constructs were generated to ensure that we were studying the function of these transporters after heterodimerization and not homodimerization. These constructs were composed of each half transporter cDNA fused with its interacting partner using the flexible linker region of P-gp, comprised of 57 amino acids (residues 703N–760D). As described by Bhatia *et al.*, this design guarantees heterodimerization but has no effect on either the localization or behavior of the transporter (34). Moreover, due to the highly flexible nature of the P-gp linker region, its structure remains elusive as it has not been solved in any of the high-resolution structures of this transporter. To assess all possible orientations, four different constructs were prepared (ABC5 $\beta$ \_P-gp linker\_ABC6, ABC6\_P-gp linker\_ABC5 $\beta$ , ABC5 $\beta$ \_P-gp linker\_ABC9, and ABC9\_P-gp linker\_ABC5 $\beta$ ). High-Five insect cells were transduced using baculovirus, encoding the aforementioned recombinant DNA, and harvested 58 to 72 h after infection. Total membrane vesicles were prepared as described in the methods section. To confirm the expression of the heterodimer chimeras in the insect cells, SDS-PAGE, followed by Coomassie-blue staining (Fig. 5A) or SDS-PAGE and Western blotting (Fig. 5B), using anti-ABC5, anti-ABC1, anti-ABC6, and anti-ABC9 antibodies, were performed. Insect cell membrane vesicles expressing only ABC5 $\beta$ , ABC6, and ABC9 were used as a control for the homodimeric form. Moreover, using site-directed mutagenesis, transporters of interest harboring an amino acid mutation in their Walker B motif of NBD were also prepared and used as negative controls. The substitution of an E with a Q abolishes in the transporter's ability to hydrolyze ATP. For the chimeric heterodimers, two different mutants were prepared, either mutation in the Walker B motif from both interacting partners or mutation only in the Walker

B from the transporter located at the C terminus. The following EQ mutants were generated: ABC5 $\beta$  E736Q, ABC6 E752Q, ABC9 E668Q, ABC5 $\beta$ \_P-gp linker\_ABC6 E736Q/E1621Q, ABC6\_P-gp linker\_ABC5 $\beta$  E752Q/E1635Q, ABC5 $\beta$ \_P-gp linker\_ABC9 E736Q/E1537Q, ABC9\_P-gp linker\_ABC5 $\beta$  E668Q/E1559Q, ABC5 $\beta$ \_P-gp linker\_ABC6 E1621Q, ABC6\_P-gp linker\_ABC5 $\beta$  E1635Q, ABC5 $\beta$ \_P-gp linker\_ABC9 E1537Q, and ABC9\_P-gp linker\_ABC5 $\beta$  E1559Q. After the preparation of total membrane vesicles from High-Five insect cells, the expression of these EQ mutants was confirmed by SDS-PAGE, followed by Coomassie-blue staining (Fig. 5A) and Western blotting (Fig. 5B). A schematic representation of the location of the mutations is shown in Figures 6A and 7A. Keniya and colleagues demonstrated the cross reactivity of anti-ABC1 (mouse monoclonal C219) with ABC5 $\beta$  (22). Figure 5C shows that anti-ABC1 was also able to recognize ABC5 $\beta$  when expressed alone or fused with its interacting partners using the P-gp linker. This is due to the significant sequence homology between the NBDs of ABC5 $\beta$  and ABC1(22). Nevertheless, ABC6 and ABC9 did not cross react with the anti-ABC1 antibody. This demonstrates that the epitope of the C219 antibody is not present in the NBDs of ABC6 or ABC9.

In Figure 5B, besides having a band at the expected molecular weight for ABC5 $\beta$ , ABC6, and ABC9 when expressed alone, at least one other band is visible at a molecular weight almost twice as high in each instance. To determine if these bands consisted of homodimers, three genetic constructs were prepared which consisted of each transporter cDNA fused with itself using the P-gp linker region resulting in chimeric homodimers (ABC5 $\beta$ \_P-gp linker\_ABC5 $\beta$ , ABC6\_P-gp linker\_ABC6, and ABC9\_P-gp linker\_ABC9). After SDS-PAGE followed by Western blotting, the chimeric homodimers were indeed seen at a similar molecular weight as the band in question (Fig. S4). This demonstrates that dimers can still be detected, confirming the correct homodimerization of ABC5 $\beta$ , ABC6, and ABC9 in insect cells.

The quantification of Coomassie-blue staining intensity of the monomer, ABC5 $\beta$ , ABC6, and ABC9 showed that these transporters are expressed at similar levels in High-Five insect cells (Fig. 6, A and B). The corresponding mutants, ABC5 $\beta$  E736Q, ABC6 E752Q, and ABC9 E668Q, also showed similar expression after Coomassie-blue staining (Fig. 6B). The different antibodies used, and their different reactivities, could explain the differences observed in the intensity of bands in Western blots. ATP hydrolysis was measured in the High-Five total membrane vesicles that expressed the homodimers, by the quantification of the inorganic phosphate released in a colorimetric assay. The three homodimers showed significant ATPase activity, which was inhibited by beryllium fluoride (BeFx) (Fig. 6C). The three transporters showed comparable ATPase activity as well as inhibition of this activity by BeFx. EQ mutants showed a decrease in ATPase activity greater than 50% (Fig. 6C). The residual ATPase activity observed in the EQ mutants was similar to that observed for control High-Five insect cells not

# ABC5β heterodimerizes with ABC6 and ABC9 in melanoma

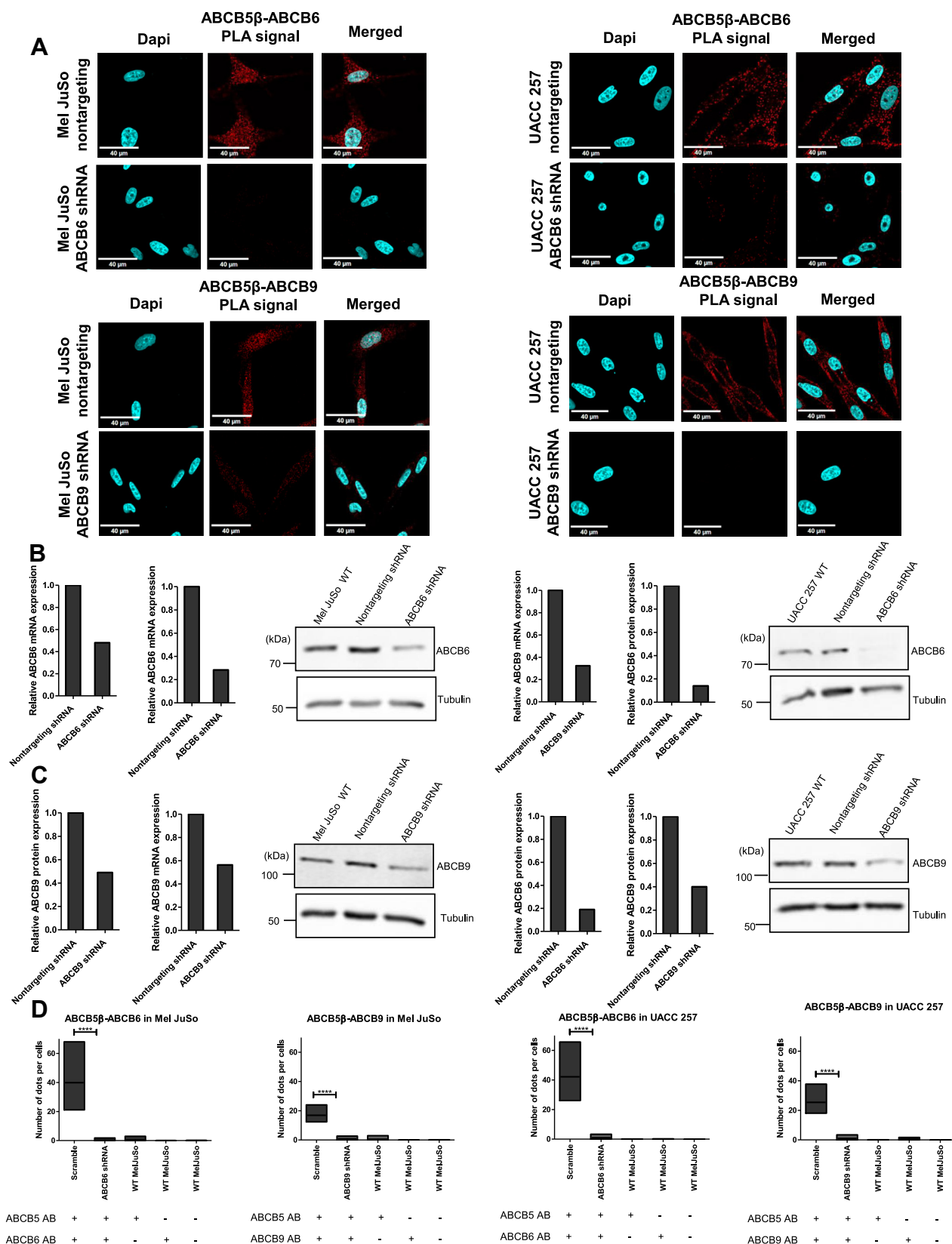


**Figure 4. Proximity ligation assay confirms the interactions between ABCB5-ABCB6 and ABCB5-ABCB9 protein pairs in Mel JuSo and UACC-257.** A, confocal images of PLA in Mel JuSo and UACC-257 that stably expressed either a nontargeting shRNA or an ABCB6-specific (or ABCB9-specific) shRNA. The detected PLA signal is in red. Nuclei are stained in blue using DAPI. The scale bar represents 40 μm. After shRNA knockdown, efficiency was determined using reverse transcription-quantitative polymerase chain reaction and Western blots in Mel JuSo (B) and UACC-257 (C). 18S and tubulin were used as references for reverse transcription-quantitative polymerase chain reaction and Western blots normalization, respectively (n = 2). ImageJ (<https://imagej.net/ij/download.html>) was used to quantify protein expression in the Western blot as well as the average number of dots per cell (n = 3) (D). Scramble

infected with baculoviruses (Fig. 6C). Therefore, this ATPase activity can be considered background noise.

On the other hand, the quantification of Coomassie-blue staining and Western blot signals revealed a difference in the heterodimer's expression levels ranging from highest to lowest as follows: ABCB5 $\beta$ \_P-gp linker\_ABCB6, ABCB6\_P-gp linker\_ABCB5 $\beta$ , ABCB9\_P-gp linker\_ABCB5 $\beta$ , and finally ABCB5 $\beta$ \_P-gp linker\_ABCB9 (Fig. 7, A and B). Similar expression was observed for their corresponding EQ mutants (Fig. 7B). It is important to note that the N terminus of ABCB6 is located on the luminal side of the membrane vesicles whereas the C terminus of ABCB5 $\beta$  is in the cytoplasm. As a result, the CCTOP two-dimensional model assumes that the fusion of ABCB5 $\beta$  when at the N terminus with ABCB6 in the C terminus leads to the trapping of one transmembrane helix from ABCB6 (TM1) in the cytoplasmic space because the P-gp linker hydrophilicity prevents it from crossing the membrane. This causes ABCB6 to lose one transmembrane helix (TM1) from its TMD0 (Fig. 7A). Nevertheless, this conformation was expressed at a high level in High-Five insect cells as compared to the three other heterodimer constructs. Interestingly, the measured ATPase activity was similar across the four heterodimeric chimeras (Fig. 7C). To determine whether the ATPase activity does actually come from the heterodimerization of our transporter of interest, the ATPase activity of the eight EQ mutants described above was analyzed. All conditions showed more than 50% decrease in ATPase activity to about the same level as observed in membrane vesicles of control High-Five cells, which confirms that most of the ATPase activity seen for the four chimeric heterodimers comes from their expression in insect cells and their heterodimerization (Fig. 7C). Moreover, no significant difference can be seen between NBDs with one mutation or a combination of mutations in both NBDs. For all the tested mutants, the decrease in BeFx-sensitive ATPase activity was due to a decrease in total ATPase activity, while the ATPase activity in the presence of BeFx remained similar to that of their unmutated counterpart. As for the monomers, the residual ATPase activity of the EQ mutants was similar to that obtained for control High-Five insect cells (Fig. 7C).

Next, ATPase activity for all the constructs was assessed in the presence of vanadate (Vi) instead of BeFx. Lower inhibition of ATPase activity was observed with 0.3 mM Vi, resulting in a lower Vi-sensitive ATPase activity than with BeFx (Fig. S5).

To visualize the potential interactions of ABCB5 $\beta$  with itself or with other transporters, three-dimensional models of the ABCB5 $\beta$  homodimer and heterodimers were constructed using the approach of homology modeling, given the availability of the crystal structure of mouse ABCB1 (PDB: 5KPI and 5KO2) and the high sequence identity between human

ABCB5 $\beta$  and mouse ABCB1, which is greater than 60% (Fig. S6). These models were further verified by coevolutionary analysis by examining interacting residues present at various domain interfaces.

The high degree of sequence identity among these transporters indicates homologous structure and function. The three-dimensional models indicate that the essential structural features of the ABCB5 $\beta$  homodimer and the ABCB5 $\beta$ /B6 and ABCB5 $\beta$ /B9 heterodimers are homologous with those of mouse P-gp. These models also show that the TMD0s of ABCB6 and ABCB9 are not engaged in the interaction of ABCB5 $\beta$  with either ABCB6 or ABCB9 (Fig. S6, B and C). Importantly, these models provide a key structural framework for further research required to determine which residues of the TMDs from ABCB5 $\beta$ , ABCB6, and ABCB9 are involved in the interaction.

## Discussion

To explore the possible role of the ABCB5 $\beta$  variant, we conducted heterodimerization studies with potential target half transporters of the ABCB family in melanoma. The ABCB family comprises three full-length transporters (*i.e.*, ABCB1, B4, and B11) and seven half transporters. ABCB5 is the only member of the ABCB family that is found as both a full transporter (ABCB5FL) and a half transporter (ABCB5 $\beta$ ), with expression driven by independent promoters. Current knowledge of these transporters led us to focus on three candidate heterodimers: ABCB5 $\beta$ -ABCB6, ABCB5 $\beta$ -ABCB8, and ABCB5 $\beta$ -ABCB9. Putative interactions between these three pairs of proteins were studied using the NanoBRET assay and confirmed using a Co-IP and PLA. Taken together, these assays revealed two novel heterodimeric ABC transporters in melanoma cell lines.

FRET microscopy in living cells has been applied to unravel the interactions of the peroxisomal ABC transporters ABCD1 and ABCD3 (35). In this study, we carried out a NanoBRET assay, which does not require extrinsic excitation and provides substantially increased detection sensitivity and dynamic range as compared to current BRET technologies (33). We demonstrated the importance of transfecting a low amount of donor and acceptor constructs to avoid either membrane crowding or protein aggregates that may lead to false positive BRET signals, as observed for ABCB8-ABCB5 $\beta$ , ABCB2-ABCD1, ABCB3-ABCD1, and ABCB5 $\beta$ -ABCD1 in Fig. S1B. This so-called bystander signal is the result of two proteins that do not interact but are close enough to transfer energy (32). The donor saturation assay confirmed the specificity of the interaction between the ABCB5 $\beta$ /B6 and ABCB5 $\beta$ /B9 protein pairs and demonstrated the nonspecificity of the interactions for the other pairs of proteins (ABCB5 $\beta$ /B8, ABCB2/D1, ABCB3/D1,

and shRNA quantifications are shown along with technical negative controls, including PLA conducted using either one antibody (AB) or none. Data is presented as mean  $\pm$  SD. In Mel JuSo: ABCB6 scramble (39.89  $\pm$  14.21), ABCB6 shRNA (0.28  $\pm$  0.60), ABCB5 AB control (0.55  $\pm$  0.91), ABCB6 AB control (0  $\pm$  0), ABCB9 scramble (16.89  $\pm$  4.27), ABCB9 shRNA (0.84  $\pm$  1.04), ABCB9 AB control (0  $\pm$  0.01), and no antibody control (0.01  $\pm$  0.05). In UACC-257: ABCB6 scramble (42.16  $\pm$  10.62), ABCB6 shRNA (0.97  $\pm$  1.00), ABCB5 AB control (0.01  $\pm$  0.02), ABCB6 AB control (0.03  $\pm$  0.07), ABCB9 scramble (25.39  $\pm$  6.74), ABCB9 shRNA (1.04  $\pm$  1.16), ABCB9 AB control (0.79  $\pm$  0.58), and no antibody control (0  $\pm$  0). Student's *t* test was performed between the scramble and shRNA conditions. Statistical significances are presented on graph as \*\*\*\**p* < 0.0001. ABCB5 $\beta$ /B6 in Mel JuSo (*t* = 9.648, *df* = 22), ABCB5 $\beta$ /B9 in Mel JuSo (*t* = 12.66, *df* = 22), ABCB5 $\beta$ /B6 in UACC-257 (*t* = 13.38, *df* = 22), ABCB5 $\beta$ /B9 in UACC-257 (*t* = 12.34, *df* = 22). DAPI, 4',6-diamidino-2-phenylindole.

## ABCB5 $\beta$ heterodimerizes with ABCB6 and ABCB9 in melanoma

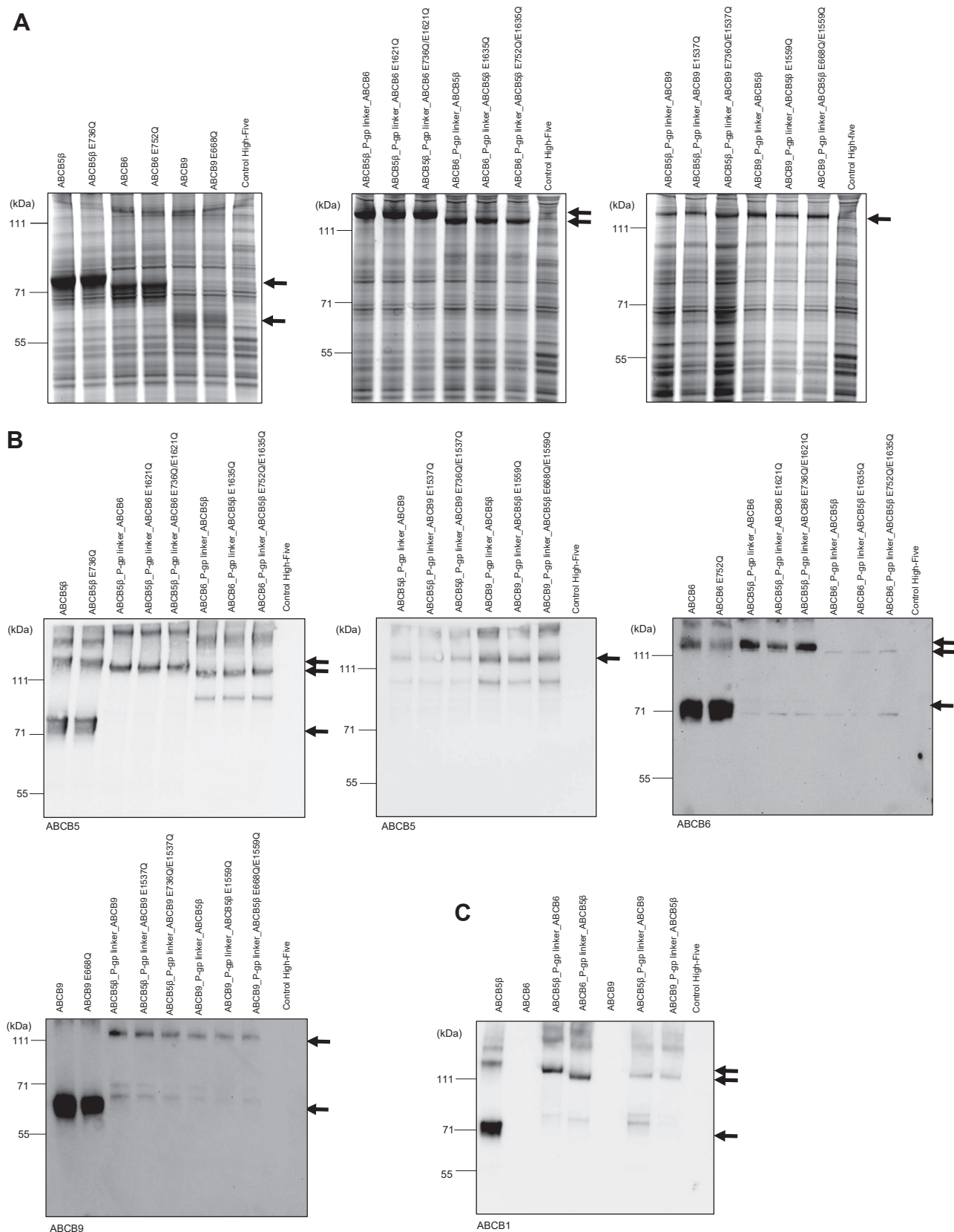


**Figure 5. Expression of ABCB5 $\beta$ , ABCB6, ABCB5 $\beta$ \_P-gp linker\_ABCB6, ABCB6\_P-gp linker\_ABCB5 $\beta$ , ABCB9, ABCB5 $\beta$ \_P-gp linker\_ABCB9, and ABCB9\_P-gp linker\_ABCB5 $\beta$  in High-Five insect cells.** Total membranes vesicles prepared from High-Five cells infected with baculovirus containing either ABCB5 $\beta$ , ABCB6, ABCB9, ABCB5 $\beta$ \_P-gp linker\_ABCB6, ABCB6\_P-gp linker\_ABCB5 $\beta$ , ABCB5 $\beta$ \_P-gp linker\_ABCB9, ABCB9\_P-gp linker\_ABCB5 $\beta$  and their corresponding EQ mutants were subjected to SDS-PAGE, followed by Coomassie-blue staining (A) or Western blotting with anti-ABCB5, anti-ABCB6, and anti-ABCB9 antibodies (B). C, Western blotting with an anti-ABCB1 antibody was performed to assess possible cross reactivity with ABCB5 $\beta$ , ABCB6, and ABCB9 and their chimeric heterodimers. Bands of interest are highlighted by black arrows.



## ABC5 $\beta$ heterodimerizes with ABC6 and ABC9 in melanoma

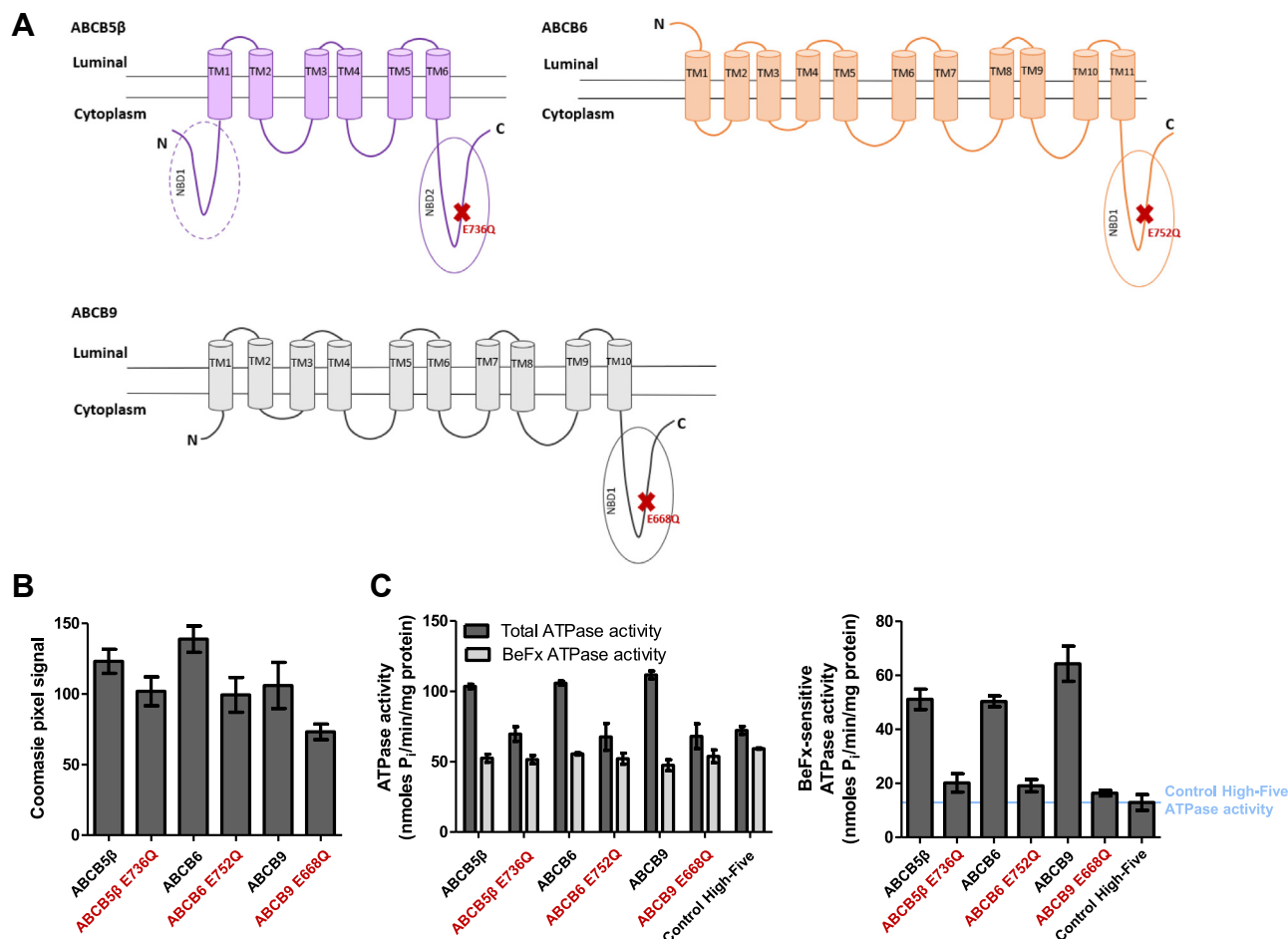


**Figure 6. Expression of homodimers in High-Five cells and BeF<sub>x</sub>-sensitive ATPase activity.** A, two-dimensional schematic representation of ABC5 $\beta$  (purple), ABC6 (orange), and ABC9 (gray) structure based on CCTOP predictions (61). ABC5 $\beta$  has one complete and another partial NBD and one TMD comprised of six transmembrane helices (TMs). The N-terminal NBD (NBD1) is truncated and lacks the conserved Walker A domain. ABC6 has six transmembrane helices (TM6-TM11) that constitute its TMD1 and five additional transmembrane helices (TM1-TM5) in the N terminus that form the TMD0. ABC9 has a TMD1 consisting of six transmembrane helices (TM5-10) and a TMD0 made of four transmembrane helices at the N terminus. The location of each EQ mutation is represented by red Xs. B, pixel intensity quantification of the protein bands of interest, after Coomassie-blue staining was performed using ImageJ (n = 3). C, ABC5 $\beta$ , ABC6, ABC9, and their corresponding EQ mutants' ATPase activities were measured in the presence and absence of BeF<sub>x</sub> as described in the methods section. On the left, data are shown as ATPase activity in the absence of BeF<sub>x</sub> (total ATPase activity) and in the presence of BeF<sub>x</sub> (BeF<sub>x</sub>-sensitive ATPase activity). On the right, data are represented by subtracting BeF<sub>x</sub>-resistant ATPase activity from the total ATPase activity (n = 3). In all panels, the names of EQ mutants are shown in red. NBD, nucleotide-binding domain; BeF<sub>x</sub>, beryllium fluoride.

and ABC5 $\beta$ /D1). Co-IP was performed to confirm the occurrence of protein-protein interaction events using the particularly easy-to-transfect HEK-293T cells. Since ABC5 $\beta$  expression had not been observed in these cells, we transfected them with mCherry-tagged ABC5 $\beta$ . This experiment allowed us to confirm the data obtained from the NanoBRET assay using the same cell line. We wanted to assess protein-protein interaction in a relevant model with a native expression of the three transporters of interest in order to avoid any potential changes in protein localization and membrane crowding caused by protein tags and protein overexpression. Since ABC5 $\beta$  is predominantly expressed in melanoma, we used two melanoma cell lines, Mel JuSo and UACC-257, which also constitutively express ABC6 and ABC9. The goal was to validate the data *in situ* in live melanoma cell lines. As such, we carried out a PLA in melanoma cell lines that stably express either a nontargeting shRNA or an ABC6-specific (or ABC9-specific) shRNA. This is the only experiment that

provides qualitative and quantitative information. The quantification of individual PLA signals, represented by red dots, revealed that ABC5 $\beta$ /B6 is more abundant than ABC5 $\beta$ /B9 in both tested cell lines. Altogether, this set of experiments demonstrates the existence of the two heterodimeric ABC transporters in the Mel JuSo and UACC-257 melanoma cell lines.

To study ABC5 $\beta$  heterodimers, four constructs were generated by fusing each of the interacting transporters with the P-gp flexible linker region in one of the two possible orientations, ABC5 $\beta$  at either the N or C terminus. After expression in High-Five insect cells, each heterodimer expression was assessed and quantified using Coomassie-blue staining and Western blotting. We found that the level of expression seems to be dependent on the orientation of each heterodimer (ABC5 $\beta$ /B6 or ABC5 $\beta$ /B9). The ABC5 $\beta$ \_P-gp linker\_ABC6 and ABC9\_P-gp linker\_ABC5 $\beta$  heterodimers are expressed at higher levels than others (see Fig. 7). It is

## ABCB5 $\beta$ heterodimerizes with ABCB6 and ABCB9 in melanoma

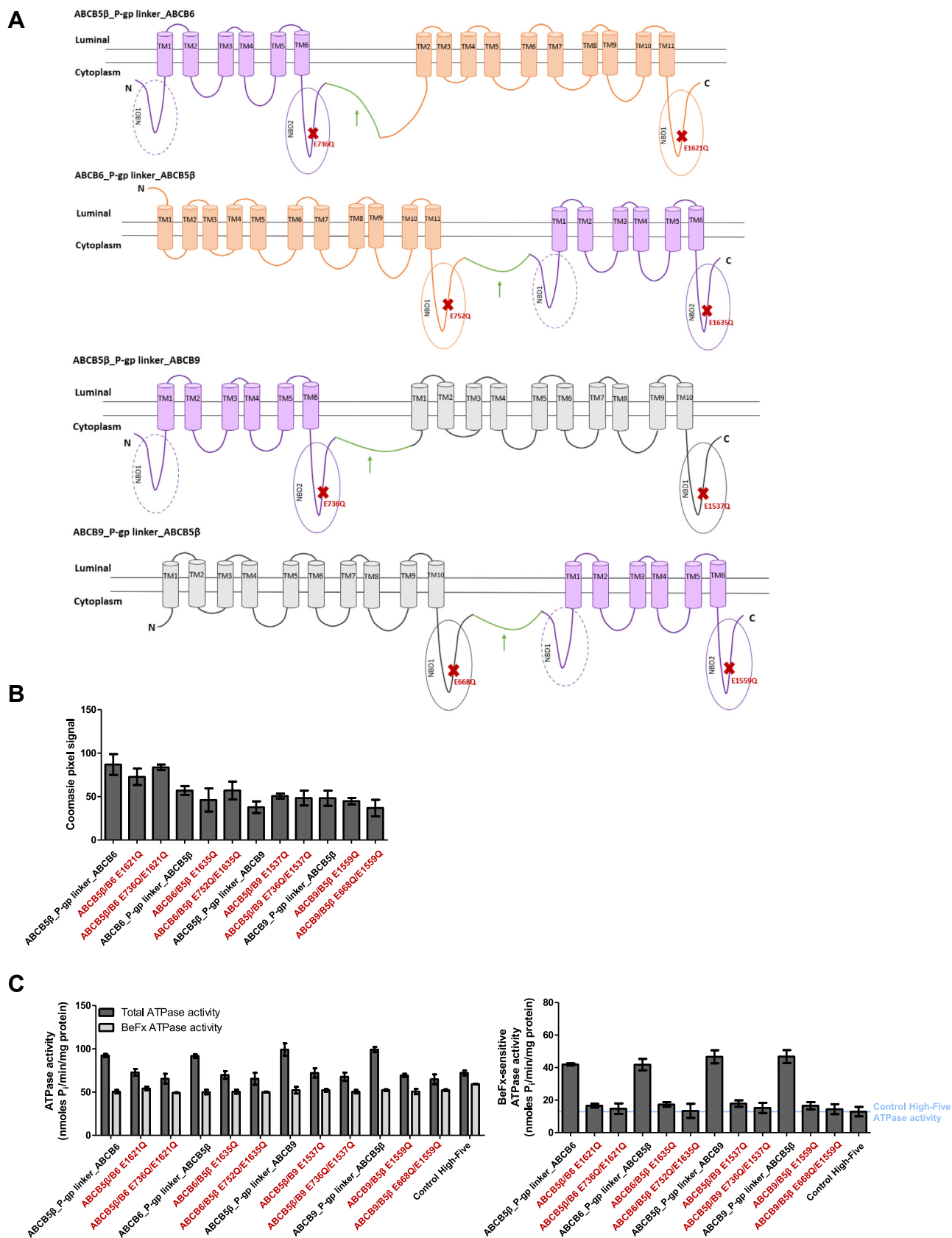


**Figure 7. Expression level and BeFx-sensitive ATPase activity of heterodimers.** A, two-dimensional schematic representation of the ABCB5 $\beta$ /B6 and ABCB5 $\beta$ /B9 heterodimers after fusion with the P-gp flexible linker based on CCTOP predictions (61). The P-gp linker is shown in green and highlighted with a green arrow; ABCB5 $\beta$  is represented in purple, ABCB6 in orange, and ABCB9 in gray. The ABCB5 $\beta$ \_P-gp linker\_ABCB6 has 16 transmembrane helices. The ABCB6\_P-gp linker\_ABCB5 $\beta$  has 17 transmembrane helices and the ABCB5 $\beta$ \_P-gp linker\_ABCB9 and ABCB9\_P-gp linker\_ABCB5 $\beta$  both have 16 transmembrane helices. The location of EQ mutations is represented by red Xs. B, the Coomassie-blue stained gel pixel intensity of the bands of interest were

important to note that, as highlighted by the CCTOP two-dimensional model, the orientation of the ABCB5 $\beta$ \_P-gp linker\_ABCB6 leads to the loss of one transmembrane helix from ABCB6 TMD0, which becomes an intracytoplasmic loop (or  $\alpha$ -helical region). However, the transmembrane localization of this helix does not seem to be required for the expression of ABCB5 $\beta$ \_P-gp linker\_ABCB6 either in insect cells or for ATPase activity. This is consistent with the three-dimensional model of ABCB5 $\beta$ /B6 and the conclusion made by Kiss and colleagues, who showed that the disruption of ABCB6 TMD0 leads to mislocalization without impairing either its dimerization or ATPase activity (36). Similar results were obtained for ABCB9 TMD0; its expression was necessary for lysosomal targeting but not for transport function or dimerization (37).

After expression in High-Five insect cells, the ATPase activity of each heterodimer was measured. In Figures 6 and 7, the ATPase activity is quantified per mg of membrane protein and is not normalized to the transporter expression. However, when considering the expression levels determined after Coomassie-blue staining quantification, ABCB5 $\beta$ \_P-gp linker\_ABCB9 displayed the highest basal ATPase activity, followed by ABCB9\_P-gp linker\_ABCB5 $\beta$ , ABCB6\_P-gp linker\_ABCB5 $\beta$ , and ABCB5 $\beta$ \_P-gp linker\_ABCB6. More experiments are needed to evaluate the influence of ABCB5 $\beta$  orientation on protein expression and ATPase activity of the heterodimers. For the homodimers, similar levels of expression and ATPase activities were observed.

To determine whether the ATPase activity observed for the homodimers and heterodimers was mediated by dimerization of the transporters and was not the result of contamination, a point mutation of a E to a Q was made in the Walker B motif of each transporter. For the heterodimers, either the C terminus Walker B was mutated or Walker B motifs in the two NBDs were mutated. All EQ mutants resulted in a significant decrease in ATPase activity, while their expression remained similar to their nonmutated counterparts. As seen in Figures 6 and 7, approximately 40% of residual ATPase activity remained after mutations in the NBDs of the transporters of interest. Part of this ATPase activity could come from the transporter itself. In fact, it is not uncommon to obtain a residual ATPase activity for EQ mutants. Janas and colleagues showed that purified NBD of Mdl1p, a homolog of the human ABC transporter TAP in *S. cerevisiae*, with an E559Q mutation, had residual ATP hydrolysis, though it was much lower than that of the WT protein (38). Similarly, the E630Q mutation in the human ABCD1 Walker B motif only resulted in a one third decrease of ATPase activity (39). In our case, only a 60% decrease is seen with the mutated transporters. Nevertheless, the residual ATPase activity is similar to that observed for the membrane vesicles of control High-Five insect cells that were not infected with baculoviruses. Therefore, this residual

ATPase activity most likely comes from other BeFx-sensitive ATPase pumps constitutively expressed in High-Five insect cells. Overall, the tested EQ mutants demonstrate that at least 60% of the ATPase activity observed is mediated by the dimers studied. Moreover, it shows that all heterodimers need two functional Walker B motifs to mediate basal ATP hydrolysis since mutation made to only the C terminus NBD of the protein also led to a similar decrease in ATPase activity. Identical observations were made for Mdr3 (mouse homolog of P-gp). Mutations in either the first Mdr3 NBD (E552Q) or the second NBD (E1125Q) both resulted in loss of ATPase activity (40).

Therefore, our results demonstrate that both heterodimers exhibit basal ATPase activity that was inhibited by BeFx, but not by vanadate. Similar results have been reported for ABCB4, ABCG1, ABCC1, and ABCC10, for which vanadate showed little to no inhibitory effect when compared to BeFx (41–43).

At this point, further investigation is needed to identify ABCB5 $\beta$ /B6 and ABCB5 $\beta$ /B9 substrates and determine whether there is any specificity in their substrate spectrum when compared to ABCB5 $\beta$ , ABCB6, and ABCB9 homodimers. It is important to point out that both ABCB6 and ABCB9 have been reported in the literature to be functional after homodimerization (44, 45). If the heterodimers also have the ability to transport substrates, it explains the similar ATPase activity obtained in our ATPase assays showing the capability of all the tested transporters to perform a complete catalytic cycle. Nevertheless, it is possible that these heterodimers have no real transport function and only exist to regulate ABCB6 and ABCB9 homodimer formation. Among the mammalian ABC transporter superfamily, previous publications have shown that ABC transporters are able to interact with different partners. For instance, using chimeric dimers, ABCD1 and ABCD2 were able to form functional homodimers, as well as heterodimers, in the peroxisome (46). In HEK293 cells, ABCG4 formed either a homodimer or heterodimer with ABCG1 (47). Nevertheless, the physiological relevance of having multiple interaction partners for ABC transporters remains unknown.

Understanding the physiological function of ABCB5 $\beta$ /B6 and ABCB5 $\beta$ /B9 heterodimers requires more study. The fact that both forms (homodimers and heterodimers) might coexist in cells, as is the case for the example mentioned above (*i.e.*, ABCD1/D2 and ABCG4/G1), remains challenging. In fact, the knock-down or downregulation of one interacting partner ultimately leads to the disappearance of both homodimers and heterodimers. Therefore, the changes observed might not be associated with their heterodimerization. Moreover, little is known about ABCB5 $\beta$  and additional investigation on this transporter is needed. Since so far, no substrates could be identified for the heterodimers, the best way to generate hypotheses about their physiological function would be to

quantified using ImageJ ( $n = 3$ ). C, the graph on the *left* shows the ATPase activity for all heterodimer chimeras and their corresponding EQ mutants measured in both the absence and presence of BeFx as described in the method section, total ATPase activity, and BeFx-sensitive ATPase activity, respectively. On the *right*, data represent BeFx-sensitive ATPase activity, which is calculated by subtracting BeFx ATPase activity from the total ATPase activity ( $n = 3$ ). In all panels, the names of EQ mutants are shown in *red*. BeFx, beryllium fluoride.

## ABCB5 $\beta$ heterodimerizes with ABCB6 and ABCB9 in melanoma

determine their localization, and such studies are currently underway.

Reports on ABCB6 localization have not been consistent; it has been shown to specifically localize to the outer membrane of the mitochondria (48) and has also been reported to localize to both the outer mitochondrial membrane and the plasma membrane (49). In a more recent study, ABCB6 was reported to have an endolysosomal localization (50). ABCB9, in contrast, was shown to go through the Golgi, be transported to endosomes and finally be trafficked to lysosomes (51). Recently, ABCB5 $\beta$  was shown to localize in the ER (52). Based on this information we can speculate that the heterodimers are localized in the ER or in lysosome-related organelles. In conclusion, this study presents the first evidence for two novel dimers with ATPase activity formed by the heterodimerization of ABCB5 $\beta$  with either ABCB6 or ABCB9 in Mel JuSo and UACC-257 melanoma cell lines. This discovery is a step toward a better understanding of the role of ABCB5 $\beta$  in melanocytes and melanoma.

### Experimental procedures

#### Cell culture and transfection

The HEK-293T cell line, which is a derivative of human embryonic kidney 293 cells, transformed with the SV40 T-antigen, and the Mel JuSo and UACC-257 melanoma cell lines were cultured in Dulbecco's modified Eagle's medium supplemented with 10% fetal bovine serum (GE Healthcare Life Sciences) and 1% penicillin/streptomycin (Gibco) at 37 °C and 5% CO<sub>2</sub> in a humidified atmosphere.

For transient transfections, cells were seeded to reach 70% confluence in a 6-well plate. Four hours later, transfection with jetPRIME (Polyplus transfection) was carried out following the manufacturer's instructions.

shRNAs constructs for the stable knockdown of human ABCB6 (sc-94721-SH) and ABCB9 (sc-60115-SH) were obtained from Santa Cruz Biotechnology. A nonsilencing shRNA was used as a control (sc-108060). Reverse transfection was performed in antibiotic-free medium with jetPRIME, following the manufacturer's instructions (Polyplus transfection). Seventy-two hours after transfection, the selection of the transfected cells was carried out by the addition of 2  $\mu$ g/ml of puromycin. After 10 days of selection, ABCB6 and ABCB9 mRNA and protein expression were assessed using reverse transcription-quantitative polymerase chain reaction and Western blot.

#### DNA constructs

For the NanoBRET constructs, ABCB2, ABCB3, ABCB5 $\beta$ , ABCB6, ABCB8, ABCB9, and ABCD1 cDNAs were inserted into the pCDNA3.1 expression vector and subcloned into the NanoLuc pNLF1-N[CMV/Hygro], the NanoLuc pNLF1-C[CMV/Hygro], the HaloTag pHTC HaloTag CMV-neo, and the HaloTag pHTN HaloTag CMV-neo vector purchased from Promega. Restriction enzymes NotI-EcoRI, NheI-EcoRI, NotI-EcoRI, and NheI-EcoRI were used, respectively.

The mCherry-tagged ABCB5 mammalian expression construct (ID: 8488-X02-787), driven by a CMV promoter, was provided by Leidos Biomedical Research (formerly SAIC-Frederick, NCI).

For the heterodimer constructs, ABCB5 $\beta$  with ABCB6 and ABCB5 $\beta$  with ABCB9 coding sequences were fused, following the NEBuilder HIFI DNA Assembly kit's instructions (New England Biolabs). The ABCB5 $\beta$ -ABCB6, ABCB6-ABCB5 $\beta$ , ABCB5 $\beta$ -ABCB9, and ABCB9-ABCB5 $\beta$  sequences were cloned in pDONR201 plasmid. Using the SmaI restriction enzyme, the sequence derived from P-gp flexible linker region residues (NEVELENAADESKSEIDALEMSSNDRSSLIRKRRS VRSQAQDRKLTKEALD) 703N-760D, was inserted between each of the half transporters. DNA sequencing was used to confirm both the correct orientation of the linker and absence of other mutations. ABCB5 $\beta$ \_P-gp linker\_ABCB6, ABCB6\_P-gp linker\_ABCB5 $\beta$ , ABCB5 $\beta$ \_P-gp linker\_ABCB9, and the ABCB9\_P-gp linker\_ABCB5 $\beta$ , ABCB5 $\beta$ , ABCB6 and ABCB9 sequences were transferred into bacmid (pDEST-008), and baculovirus was generated by the Protein Expression Laboratory Cloning and Optimization Group (Frederick National Laboratory for Cancer Research).

The EQ mutations in the Walker B domain of one or both NBDs of transporters were prepared using Q5 site-directed mutagenesis following the manufacturer's instructions (New England Biolabs). Mutated cDNAs were transferred into bacmid (pDEST-008), and baculoviruses were generated by the Protein Expression Laboratory Cloning and Optimization Group (Frederick National Laboratory for Cancer Research).

#### Reverse transcription-quantitative polymerase chain reaction

Total RNA was isolated from Mel JuSo and UACC-257 using a NucleoSpin RNA Plus kit following the manufacturer's instructions (Takarabio). Reverse transcription was performed using a High-Capacity cDNA Reverse Transcription kit and 200 ng of total RNA (Thermo Fisher Scientific) according to the manufacturer's instructions. Quantitative PCR was performed using TaqMan master mix (Thermo Fisher Scientific) and 18s expression was used to normalize data. The following probes from Thermo Fisher Scientific were used: 18S (Hs03003631\_g1), ABCB6 (Hs00180568\_m1), and ABCB9 (Hs00608640\_m1).

#### Nanoluciferase-based bioluminescence resonance energy transfer

Twenty-four hours after the transient transfection of the NanoLuc and HaloTag constructs, the cells were washed with PBS and trypsinized. Cells were counted and diluted in Opti-MEM supplemented with 4% fetal bovine serum to reach a density of  $2 \times 10^5$  cells/ml. One microliter of 0.1 mM HaloTag NanoBRET ligand 618 (Promega) per ml of cells, or DMSO in the control conditions, was added. One hundred microliters of cells with either ligand or DMSO were plated in a 96-well plate (Corning 3917, Thermo Fisher Scientific) and were cultured overnight at 37 °C, 5% CO<sub>2</sub>. Twenty-five microliters of 100 $\times$  dilution of NanoBRET NanoGlo substrate (Promega) was

added per well. Plates were shaken for 30 s at 400 rpm and then kept in the dark for 30 s. Finally, donor emission (447 nm) and acceptor emission (610 nm) were measured at room temperature using a dual filter (SpectraMax i3x, Molecular Devices). For all experiments, biological triplicates were performed. All biological triplicates were composed of technical triplicates.

Relative light units obtained for donor and acceptor emission were processed as follows to obtain milli bioluminescence units:

$$\frac{\text{emission 610 nm}}{\text{emission 447 nm}} = BU \times 1000 = mBU$$

For saturation experiments, percentages of the maximum NanoBRET ratio were plotted against the acceptor to donor ratio; data were fitted using the “one site–total and nonspecific binding” fit in Prism.

### Coimmunoprecipitation

Five milligrams of total protein (from either HEK93T, Mel Juso, or UACC-257) in lysis buffer (120 mM NaCl, 50 mM Tris, NP40 0.5%, 5 mM EDTA, 1 $\times$  protease inhibitor) were incubated on a rotating wheel at 4 °C for 4 h with 1  $\mu$ g of antibody: ABCB5 (600-401-A775, Rockland Immunochemicals), ABCB6 (G-10, Santa Cruz Biotechnology), ABCB9 (A-8, Santa Cruz Biotechnology), IgG Mouse (sc-2025, Santa Cruz Biotechnology, Dalla), and IgG Rabbit (sc-3888, Santa Cruz Biotechnology). Simultaneously, 25  $\mu$ l of magnetic beads, Dynabeads-Protein A (Invitrogen), and Dynabeads-Protein G (Invitrogen) were added to an Eppendorf and washed twice with 250  $\mu$ l of lysis buffer using a magnetic rack. Thereafter, protein lysates with the antibody were added to the beads and incubated overnight at 4 °C on a rotating wheel. The following day, the beads were washed three times with 250  $\mu$ l of cold PBS 0.05% Tween 20. Fifty microliters of elution buffer (DTT, Tris, Glycerol, SDS) were added, and samples were heated at 40 °C for 10 min. Samples were then analyzed using Western blot.

### SDS-PAGE and western blotting after Co-IP

Samples were loaded on an 8% SDS acrylamide gel, migrated at 110 V, and transferred to a polyvinylidene difluoride membrane at 110 V for 1 h 30 mins. The membrane was blocked for 1 h in 5% milk diluted in PBS 0.05% Tween 20 and incubated overnight with the following primary antibodies: anti-ABCB5 (600-401-A775, Rockland Immunochemicals), anti-ABCB6 (sc-365930, Santa Cruz Biotechnology), anti-ABCB9 (sc-39412, Santa Cruz Biotechnology), and anti-mCherry (ab167453, Abcam). Then, membranes were incubated for 1 h with either Scan Later anti-mouse or anti-rabbit secondary antibodies (Molecular Devices); they were then washed with PBS 0.05% Tween 20 and revealed with the SpectraMax i3x (Molecular Devices). Alternatively, membranes were incubated for 1 h with horseradish peroxidase–conjugated goat anti-mouse or anti-rabbit antibodies (Agilent Technologies),

washed with PBS 0.05% Tween, and revealed with enhanced chemiluminescence (PerkinElmer).

### In situ PLA

Cells grown on a coverslip were fixed in 4% paraformaldehyde for 20 min and permeabilized with PBS + Triton X-100 0.2% for 10 min. Then, a PLA was performed in accordance with the Duolink kit (Sigma-Aldrich). Briefly, the coverslips were incubated with blocking solution for 1 h at 37 °C in a humidity chamber. Then, they were incubated for 1 h at room temperature with primary antibody pairs raised against different species (mouse and rabbit) and diluted 1/200: ABCB5 $\beta$  (LS-C169144, LSBio), ABCB6 (600-401-945, Rockland Immunochemicals), ABCB8 (ab83194, Abcam), and ABCB9 (PA5-99017, Invitrogen). Cells were incubated with PLA probes mouse PLUS and rabbit MINUS for 1 h at 37 °C. Next, ligation was performed for 30 min at 37 °C, followed by amplification for 100 min at 37 °C. Finally, the coverslips were mounted on mounting medium with 4',6-diamidino-2-phenylindole (Sigma-Aldrich). The edges were sealed with clear nail polish. Images were obtained using a Leica TCS SP5 confocal microscope (Leica Microsystems). 4',6-diamidino-2-phenylindole, argon, and 561 red filters were used. The number of red dots per cell was counted using ImageJ software as described in Gomes *et al* (53). Each condition was obtained in biological triplicates.

### Structural homology models of ABCB5 $\beta$ homodimer and heterodimers

An accurate alignment between the human ABCB5 $\beta$  and mouse ABCB1 sequences was generated based on a multi-sequence alignment that includes various members of the ABCB family transporters. Based on this alignment, a structural model of ABCB5 $\beta$  was constructed manually using the structural model of mouse P-gp (PDB:5KPI) (54) as a template, replacing the residues of mouse ABCB1 with the corresponding residues of ABCB5 $\beta$  in the molecular graphics program Coot (55). The model was subsequently subject to energy minimization using the crystallographic refinement program Refmac (56).

The construction of the heterodimeric ABCB5 $\beta$ -ABCB6 model was initiated using a dimeric cryo-EM model of ABCB6 (PDB:7D7N) (57). A single monomer model of ABCB6 was superposed to the corresponding subunit of the ABCB5 $\beta$  dimer model. Manual adjustments were made to make sure all helices were correctly aligned with the NBDs using the molecular modeling program Coot. The model was then energy minimized using the crystallographic refinement program Refmac. The ABCB5 $\beta$ -ABCB6 model was rendered as ribbon diagram in the program PyMol (<https://pymol.org/2/>) (58).

The construction of the ABCB5 $\beta$  and ABCB9 heterodimeric model started with the construction of the homology model of ABCB9. The ABCB9 sequence was aligned with that of ABCB6. Mutations were manually introduced into the ABCB6 subunit of the ABCB5 $\beta$ -ABCB6 model based on the sequence alignment in Coot. The resulting ABCB5 $\beta$ -ABCB9 model was then subjected to several cycles of energy minimization.

## ABCB5 $\beta$ heterodimerizes with ABCB6 and ABCB9 in melanoma

### Insect cell total membrane preparation

*Trichoplusia ni* (High-Five) insect cells were infected at a multiplicity of infection of 10 with a recombinant baculovirus carrying one of the following sequences: ABCB5 $\beta$ , ABCB6, ABCB9, ABCB5 $\beta$ \_P-gp linker\_ABCB6, ABCB6\_P-gp linker\_ABCB5 $\beta$ , ABCB5 $\beta$ \_P-gp linker\_ABCB9, ABCB9\_P-gp linker\_ABCB5 $\beta$ , and their corresponding EQ mutants. Cells were harvested after 58 to 72 h, washed with PBS containing 1% aprotinin, and stored at  $-80^{\circ}\text{C}$ . Total membrane vesicles were prepared with hypotonic lysis and differential centrifugation as detailed in (59).

### SDS-PAGE and Western blotting of insect cells membrane vesicles

After incubation in loading dye (500 mM Tris-HCl pH 6.8, 10% SDS, 30% sucrose, 0.005% bromophenol blue, and 25%  $\beta$  mercaptoethanol) at  $37^{\circ}\text{C}$  for 20 min, total membrane vesicles were electrophoresed on a 7% NuPAGE precast gel (Invitrogen) for 1 h 10 mins at 150 V. Then gels were either stained with Coomassie-blue (15  $\mu\text{g}$  of protein per lane) (Instant blue, Abcam) or transferred to nitrocellulose membranes (0.25  $\mu\text{g}$  or 1  $\mu\text{g}$  of protein per lane for the monomeric transporters and heterodimer, respectively) and probed with the following primary antibodies overnight at  $4^{\circ}\text{C}$ : anti-ABCB5 (600-401-A775, Rockland Immunochemicals), anti-ABCB1 (C219, Fujirebio), anti-ABCB6 (sc-365930, Santa Cruz Biotechnology), anti-ABCB9 (sc-39412, Santa Cruz Biotechnology). Then, nitrocellulose membranes were incubated with horseradish peroxidase-conjugated goat anti-mouse secondary (Santa Cruz Biotechnology) for 1 h at room temperature and revealed using ChemiDoc (Bio-Rad, Hercules).

### ATPase assay

Total membrane vesicles prepared from High-Five insect cells were diluted in ATPase assay buffer (50 mM MES-Tris pH 6.8, 50 mM KCl, 5 mM sodium azide, 1 mM EGTA, 1 mM ouabain, 10 mM  $\text{MgCl}_2$ , 2 mM DTT) to reach a final concentration of 10  $\mu\text{g}$  protein/0.1 ml. The reaction was started with the addition of 5 mM ATP and was performed at  $37^{\circ}\text{C}$  for 20 min. After 20 min, the reaction was terminated with 0.1 ml of 10% SDS. The amount of inorganic phosphate released was measured in both the presence and the absence of Vi (0.3 mM) and BeFx (0.2 mM beryllium sulfate and 2.5 mM sodium fluoride) using a colorimetric method described in (60).

### Statistical analysis

Data were analyzed using GraphPad Prism (<https://www.graphpad.com>) version 5.04 for Windows with either linear regression or an unpaired Student's *t* test. Statistical analysis is described in the figure legends. Statistical significance was defined as  $p < 0.05$ . All data are contained within the manuscript.

**Supporting information**—The article contains supporting information.

**Acknowledgments**—We would like to thank Simon Lefèvre for his initial work on coimmunoprecipitations, and Andy Cheigné of the Department of Infection and Immunity, Luxembourg Institute of Health, for the useful conversation regarding NanoBRET experiments. We are grateful to Vincent Van Hée and Marylène Focant of Promega for their support in the optimization and troubleshooting of the NanoBRET assay. We would also like to thank Marielle Boonen (Intracellular Trafficking Biology, NARILIS, UNamur) for her critical reading of the manuscript. We thank George Leiman for editorial help.

**Author contributions**—L. G., L. D., D. X., S. V. A., M. M. G., and J. P.-G. conceptualization; L. G., L. D., P. S., D. X., S. V. A., and J. P.-G. methodology; L. G., L. D., M. F., P. S., L. S., and D. X. investigation; L. G., D. X., S. V. A. M. M. G. and J.-P. G. formal analysis; L. G. writing-original draft; S. V. A., and J.-P. G. supervision; L. G., P. S., D. X., S. V. A., M. M. G., and J. P. G. writing-reviewing and editing; J.-P. G. data curation.

**Funding and additional information**—P. S., D. X., S. V. A., and M. M. G. were supported by the Intramural Program of the National Institutes of Health, National Cancer Institute, Center for Cancer Research. The content is solely the responsibility of the authors and does not necessarily represent the official views of the National Institutes of Health.

**Conflict of interest**—The authors declare that they have no conflicts of interest with the contents of this article.

**Abbreviations**—The abbreviations used are: BeFx, beryllium fluoride; cDNA, complementary deoxyribonucleic acid; Co-IP, coimmunoprecipitation; DMSO, dimethyl sulfoxide; ER, endoplasmic reticulum; NanoBRET, nanoluciferase-based bioluminescence resonance energy transfer; NBD, nucleotide-binding domain; PLA, proximity ligation assay; TMD, transmembrane domain.

### References

1. Thomas, C., and Tampe, R. (2020) Structural and mechanistic principles of ABC transporters. *Annu. Rev. Biochem.* **89**, 605–636
2. Molday, R. S., Garces, F. A., Scortecci, J. F., and Molday, L. L. (2021) Structure and function of ABCA4 and its role in the visual cycle and Stargardt macular degeneration. *Prog. Retin. Eye Res.* <https://doi.org/10.1016/j.preteyeres.2021.101036>
3. Kawaguchi, K., and Morita, M. (2016) ABC transporter subfamily D: distinct differences in behavior between ABCD1-3 and ABCD4 in subcellular localization, function, and human disease. *Biomed. Res. Int.* **2016**, 6786245
4. Gerovac, M., and Tampe, R. (2019) Control of mRNA translation by versatile ATP-driven machines trends. *Biochem. Sci.* **44**, 167–180
5. Csanady, L., Vergani, P., and Gadsby, D. C. (2019) Structure, gating, and regulation of the Cl<sup>-</sup> anion channel. *Physiol. Rev.* **99**, 707–738
6. Tinker, A., Aziz, Q., Li, Y., and Specterman, M. (2018) ATP-sensitive potassium channels and their physiological and pathophysiological roles. *Compr. Physiol.* **8**, 1463–1511
7. Frank, N. Y., Pendse, S. S., Lapchak, P. H., Margaryan, A., Shlain, D., Doeing, C., et al. (2003) Regulation of progenitor cell fusion by ABCB5 P-glycoprotein, a novel human ATP-binding cassette transporter. *J. Biol. Chem.* **278**, 47156–47165
8. Schatton, T., Murphy, G. F., Frank, N. Y., Yamaura, K., Waaga-Gasser, A. M., Gasser, M., et al. (2008) Identification of cells initiating human melanomas. *Nature* **451**, 345–349
9. Ksander, B. R., Kolovou, P. E., Wilson, B. J., Saab, K. R., Guo, Q., Ma, J., et al. (2014) ABCB5 is a limbal stem cell gene required for corneal development and repair. *Nature* **511**, 353–357

10. Frank, N. Y., Margaryan, A., Huang, Y., Schatton, T., Waaga-Gasser, A. M., Gasser, M., *et al.* (2005) ABCB5-mediated doxorubicin transport and chemoresistance in human malignant melanoma. *Cancer Res.* **65**, 4320–4333
11. Yang, J. Y., Ha, S. A., Yang, Y. S., and Kim, J. W. (2010) Glycoprotein ABCB5 and YB-1 expression plays a role in increased heterogeneity of breast cancer cells: correlations with cell fusion and doxorubicin resistance. *BMC Cancer* **10**, 388
12. Wilson, B. J., Schatton, T., Zhan, Q., Gasser, M., Ma, J., Saab, K. R., *et al.* (2011) ABCB5 identifies a therapy-refractory tumor cell population in colorectal cancer patients. *Cancer Res.* **71**, 5307–5316
13. Kugimiya, N., Nishimoto, A., Hosoyama, T., Ueno, K., Enoki, T., Li, T. S., *et al.* (2015) The c-MYC-ABCB5 axis plays a pivotal role in 5-fluorouracil resistance in human colon cancer cells. *J. Cell Mol. Med.* **19**, 1569–1581
14. Cheung, S. T., Cheung, P. F., Cheng, C. K., Wong, N. C., and Fan, S. T. (2011) Granulin-epithelin precursor and ATP-dependent binding cassette (ABC)B5 regulate liver cancer cell chemoresistance. *Gastroenterology* **140**, 344–355
15. Farawela, H. M., Khorshied, M. M., Kassem, N. M., Kassem, H. A., and Zawam, H. M. (2014) The clinical relevance and prognostic significance of adenosine triphosphate ATP-binding cassette (ABCB5) and multidrug resistance (MDR1) genes expression in acute leukemia: an Egyptian study. *J. Cancer Res. Clin. Oncol.* **140**, 1323–1330
16. Yang, M., Li, W., Fan, D., Yan, Y., Zhang, X., Zhang, Y., *et al.* (2012) Expression of ABCB5 gene in hematological malignancies and its significance. *Leuk. Lymphoma* **53**, 1211–1215
17. Thierry-Mieg, D., and Thierry-Mieg, J. (2006) AceView: a comprehensive cDNA-supported gene and transcripts annotation. *Genome Biol.* **7**, 11–14
18. Chen, K. G., Szakacs, G., Annereau, J. P., Rouzaud, F., Liang, X. J., Valencia, J. C., *et al.* (2005) Principal expression of two mRNA isoforms (ABCB 5 $\alpha$  and ABCB 5 $\beta$ ) of the ATP-binding cassette transporter gene ABCB 5 in melanoma cells and melanocytes. *Pigment Cell Res.* **18**, 102–112
19. Kawanobe, T., Kogure, S., Nakamura, S., Sato, M., Katayama, K., Mitsuhashi, J., *et al.* (2012) Expression of human ABCB5 confers resistance to taxanes and anthracyclines. *Biochem. Biophys. Res. Commun.* **418**, 736–741
20. Moitra, K., Im, K., Limpert, K., Borsa, A., Sawitzke, J., Robey, R., *et al.* (2012) Differential gene and microRNA expression between etoposide resistant and etoposide sensitive MCF7 breast cancer cell lines. *PLoS One* **7**, e45268
21. Gillet, J. P., Efferth, T., and Remacle, J. (2007) Chemotherapy-induced resistance by ATP-binding cassette transporter genes. *Biochim. Biophys. Acta* **1775**, 237–262
22. Keniya, M. V., Holmes, A. R., Niimi, M., Lamping, E., Gillet, J. P., Gottesman, M. M., *et al.* (2014) Drug resistance is conferred on the model yeast *Saccharomyces cerevisiae* by expression of full-length melanoma-associated human ATP-binding cassette transporter Abcb5. *Mol. Pharm.* **11**, 3452–3462
23. Urlinger, S., Kuchler, K., Meyer, T. H., Uebel, S., and Tampé, R. (1997) Intracellular location, complex formation, and function of the transporter associated with antigen processing in yeast. *Eur. J. Biochem.* **245**, 266–272
24. Maio, N., Kim, K. S., Holmes-Hampton, G., Singh, A., and Rouault, T. A. (2019) Dimeric ferrochelatase bridges ABCB7 and ABCB10 homodimers in an architecturally defined molecular complex required for heme biosynthesis. *Haematologica* **104**, 1756–1767
25. Elliott, A. M., and Al-Hajj, M. A. (2009) ABCB8 mediates doxorubicin resistance in melanoma cells by protecting the mitochondrial genome. *Mol. Cancer Res.* **7**, 79–87
26. Minami, K., Kamijo, Y., Nishizawa, Y., Tabata, S., Horikuchi, F., Yamamoto, M., *et al.* (2014) Expression of ABCB6 is related to resistance to 5-FU, SN-38 and vincristine. *Anticancer Res.* **34**, 4767–4773
27. Gong, J.-P., Yang, L., Tang, J.-W., Sun, P., Hu, Q., Qin, J.-W., *et al.* (2016) Overexpression of microRNA-24 increases the sensitivity to paclitaxel in drug-resistant breast carcinoma cell lines *via* targeting Abcb9. *Oncol. Lett.* **12**, 3905–3911
28. Bergam, P., Reisecker, J. M., Rakvac, Z., Kucsma, N., Raposo, G., Szakacs, G., *et al.* (2018) ABCB6 resides in melanosomes and regulates early steps of melanogenesis required for PMEL amyloid matrix formation. *J. Mol. Biol.* **430**, 3802–3818
29. Zhang, C., Li, D., Zhang, J., Chen, X., Huang, M., Archacki, S., *et al.* (2013) Mutations in ABCB6 cause dyschromatosis universalis hereditaria. *J. Invest. Dermatol.* **133**, 2221–2228
30. Chen, K. G., Valencia, J. C., Gillet, J.-P., Hearing, V. J., and Gottesman, M. M. (2010) Involvement of ABC transporters in melanogenesis and the development of multidrug resistance of melanoma. *Pigment Cell Melanoma Res.* **22**, 740–749
31. Chen, K. G., Valencia, J. C., Lai, B., Zhang, G., Paterson, J. K., Rouzaud, F., *et al.* (2006) Melanosomal sequestration of cytotoxic drugs contributes to the intractability of malignant melanomas. *Proc. Natl. Acad. Sci. U. S. A.* **103**, 9903–9907
32. King, C., Raicu, V., and Hristova, K. (2017) Understanding the FRET signatures of interacting membrane proteins. *J. Biol. Chem.* **292**, 5291–5310
33. Machleidt, T., Woodroffe, C. C., Schwinn, M. K., Mendez, J., Robers, M. B., Zimmerman, K., *et al.* (2015) NanoBRET - a novel platform for the analysis of protein-protein interactions. *ACS Chem. Biol.* **10**, 1797–1804
34. Bhatia, A., Schafer, H., and Hrycyna, C. (2005) Oligomerization of the human ABC transporter ABCG2: evaluation of the native protein and chimeric dimers. *Biochemistry* **44**, 10893–10904
35. Hillebrand, M., Verrier, S. E., Ohlenbusch, A., Schafer, A., Soling, H. D., Wouters, F. S., *et al.* (2007) Live cell FRET microscopy: homo- and heterodimerization of two human peroxisomal ABC transporters, the adrenoleukodystrophy protein (ALDP, ABCD1) and PMP70 (ABCD3). *J. Biol. Chem.* **282**, 26997–27005
36. Kiss, K., Kucsma, N., Brozik, A., Tusnady, E., Bergam, P., Van Niel, G., *et al.* (2015) Role of the N-terminal transmembrane domain in the endolysosomal targeting and function of the human ABCB6 protein. *Biochem. J.* **467**, 127–139
37. Demirel, O., Bangert, I., Tampé, R., and Abele, R. (2010) Tuning the cellular trafficking of the lysosomal peptide transporter TAPL by its N-terminal domain. *Traffic* **11**, 383–393
38. Janas, E., Hofacker, M., Chen, M., Gompf, S., van der Does, C., and Tampé, R. (2003) The ATP hydrolysis cycle of the nucleotide-binding domain of the mitochondrial ATP-binding cassette transporter Mdl1p. *J. Biol. Chem.* **278**, 26862–26869
39. Xiong, C., Jia, L.-N., Xiong, W.-X., Wu, X.-T., Xiong, L.-L., Wang, T.-H., *et al.* (2023) Structural insights into substrate recognition and translocation of human peroxisomal ABC transporter ALDP. *Nature* **8**, 74
40. Urbatsch, I. L., Julien, M., Carrier, I., Rousseau, M.-E., Cayrol, R., and Gros, P. (2000) Mutational analysis of conserved carboxylate residues in the nucleotide binding sites of P-glycoprotein. *Biochemistry* **39**, 14138–14149
41. Kluth, M., Stindt, J., Droge, C., Linnemann, D., Kubitz, R., and Schmitt, L. (2015) A mutation within the extended X loop abolished substrate-induced ATPase activity of the human liver ATP-binding cassette (ABC) transporter MDR3. *J. Biol. Chem.* **290**, 4896–4907
42. Hirayama, H., Kimura, Y., Matsuo, M., and Ueda, K. (2013) ATPase activity of human ABCG1 is stimulated by cholesterol and sphingomyelin. *J. Lipid Res.* **54**, 496–502
43. Malofeeva, E., Domanitskaya, N., Gudima, M., and Hopper-Borge, E. (2013) Modulation of the ATPase and transport activities of broad-acting multidrug resistance factor ABCC0 (MRP7). *Cancer Res.* **72**, 6457–6467
44. Chavan, H., Khan, M. M., Tegos, G., and Krishnamurthy, P. (2013) Efficient purification and reconstitution of ATP binding cassette transporter B6 (ABCB6) for functional and structural studies. *J. Biol. Chem.* **288**, 22658–22669
45. Ohara, T., Ohashi-Kobayashi, A., and Maeda, M. (2008) Biochemical characterization of transporter associated with antigen processing (TAP)-like (ABCB9) expressed in insect cells. *Biol. Pharm. Bull.* **31**, 1–5
46. Geillon, F., Gondcaille, C., Charbonnier, S., Van Roermund, C., Lopez, T., Dias, A., *et al.* (2014) Structure-function analysis of peroxisomal ATP-binding cassette transporters using chimeric dimers. *J. Biol. Chem.* **289**, 24511–24520
47. Hegyi, Z., and Homolya, L. (2016) Functional cooperativity between ABCG4 and ABCG1 isoforms. *PLoS One* **11**, e0156516
48. Krishnamurthy, P. C., Du, G., Fukuda, Y., Sun, D., Sampath, J., Mercer, K. E., *et al.* (2006) Identification of a mammalian mitochondrial porphyrin transporter. *Nature* **443**, 586–589

## ABCB5 $\beta$ heterodimerizes with ABCB6 and ABCB9 in melanoma

49. Paterson, J. K., Shukla, S., Black, C. M., Tachiwada, T., Garfield, S., Wincovitch, S., *et al.* (2007) Human ABCB6 localizes to both the outer mitochondrial membrane and the plasma membrane. *Biochemistry* **46**, 9443–9452
50. Kiss, K., Brozik, A., Kucsma, N., Toth, A., Gera, M., Berry, L., *et al.* (2012) Shifting the paradigm: the putative mitochondrial protein ABCB6 resides in the lysosomes of cells and in the plasma membrane of erythrocytes. *PLoS One* **7**, e37378
51. Graab, P., Bock, C., Weiss, K., Hirth, A., Koller, N., Braner, M., *et al.* (2019) Lysosomal targeting of the ABC transporter TAPL is determined by membrane-localized charged residues. *J. Biol. Chem.* **294**, 7308–7323
52. Adriana, D.-A., Gerard, L., Albert, M., Gaussin, J.-F., Boonen, M., and Gillet, J.-P. (2023) The  $\beta$  isoform of human ATP-binding cassette B5 transporter, ABCB5 $\beta$ , localizes to the endoplasmic reticulum. *Int. J. Mol. Sci.* **24**, 15847
53. Gomes, I., Sierra, S., and Devi, L. A. (2016) Detection of receptor heterodimerization using *in situ* proximity ligation assay. *Curr. Protoc. Pharmacol.* **75**. <https://doi.org/10.1002/cpph.15>
54. Esser, L., Zhou, F., Pluchino, K. M., Shiloach, J., Ma, J., Tang, W. K., *et al.* (2017) Structures of the multidrug transporter P-glycoprotein reveal asymmetric ATP binding and the mechanism of polyspecificity. *J. Biol. Chem.* **292**, 446–461
55. Emsley, P., and Cowtan, K. (2004) Coot: model-building tools for molecular graphics. *Acta Crystallogr. D Biol. Crystallogr.* **60**, 2126–2132
56. Murshudov, G. N., Vagin, A. A., and Dodson, E. J. (1997) Refinement of macromolecular structures by the maximum-likelihood method. *Acta Crystallogr. D Biol. Crystallogr.* **53**, 240–255
57. Wang, C., Cao, C., Wang, N., Wang, X., Wang, X., and Zhang, X. C. (2020) Cryo-electron microscopy structure of human ABCB6 transporter. *Protein Sci.* **29**, 2363–2374
58. DeLano, W. L. (2002) Pymol: an open-source molecular graphics tool. *CCP4 Newsletter on protein. Crystallography* **40**, 82–92
59. Nandigama, K., Lusvarghi, S., Shukla, S., and Ambudkar, S. (2019) Large-scale purification of functional human P-glycoprotein (ABCB1). *Protein. Expr. Purif.* **159**, 60–68
60. Ambudkar, S. V. (1998) Drug-stimulatable ATPase activity in crude membranes of human MDR1-transfected mammalian cells. *Methods Enzymol.* **292**, 504–514
61. Dobson, L., Remenyi, I., and Tusnady, E. (2015) Cctop : a consensus constrained TOPology prediction web server. *Nucleic Acids Res.* **43**, W408–W412